THE JOURNAL OF PHYSICAL CHEMISTRY B
A JOURNAL OF THE AMERICAN CHEMICAL SOCIETY

pubs.acs.org/JPCB

Article

The Interaction of NF-κB Transcription Factor with Centromeric Chromatin

Shaun Filliaux, Chloe Bertelsen, Hannah Baughman, Elizabeth Komives,* and Yuri Lyubchenko*

Cite This: https://doi.org/10.1021/acs.jpcb.3c08388

Read Online

ACCESS | Metrics & More | Article Recommendations | Supporting Information

ABSTRACT: Centromeric chromatin is a subset of chromatin structure and governs chromosome segregation. The centromere is composed of both CENP-A nucleosomes (CENP-A_{nuc}) and H3 nucleosomes ($H3_{nuc}$) and is enriched with alpha-satellite (α-sat) DNA repeats. These CENP-A_{nuc} have a different structure than $H3_{nuc}$, decreasing the base pairs (bp) of wrapped DNA from 147 bp for $H3_{nuc}$ to 121 bp for CENP-A_{nuc}. All these factors can contribute to centromere function. We investigated the interaction of $H3_{nuc}$ and CENP-A_{nuc} with NF-κB, a crucial transcription factor in regulating immune response and inflammation. We utilized atomic force microscopy (AFM) to characterize complexes of both types of nucleosomes with NF-κB. We found that NF-κB unravels $H3_{nuc}$, removing more than 20 bp of DNA, and that NF-κB binds to the nucleosomal core. Similar results were obtained for the truncated variant of NF-κB comprised only of the Rel homology domain and missing the transcription activation domain (TAD), suggesting that $RelA_{TAD}$ is not critical in unraveling $H3_{nuc}$. By contrast, NF-κB did not bind to or unravel CENP-A_{nuc}. These findings with different affinities for two types of nucleosomes to NF-κB may have implications for understanding the mechanisms of gene expression in bulk and centromere chromatin.

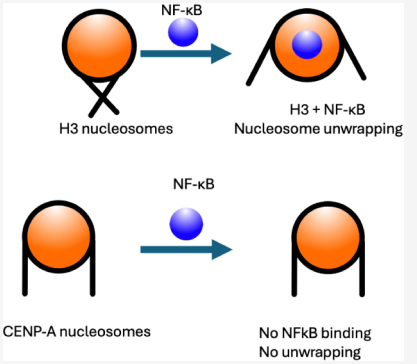

INTRODUCTION

The centromere is a specialized chromatin region located at the center of each eukaryotic chromosome and is responsible for ensuring proper segregation during mitosis and meiosis.[1] It consists of a complex network of proteins, DNA sequences, and chromatin structures that interact to form a cohesive unit responsible for accurately segregating chromosomes performed by the kinetochores.[2,3] Although bulk chromatin consists of one type of nucleosomes with octamers consisting of duplicates of H2A, H2B, H3, and H4 histones (nucleosome $H3_{nuc}$), centromere chromatin consists of two types of nucleosomes CENP-A (CENP-A_{nuc}) and canonical $H3_{nuc}$ nucleosomes.[4] The only difference between these two nucleosomes is that in $H3_{nuc}$, histones are replaced with variant CENP-A histones. The centromere of most higher eukaryotes is comprised of alpha satellite (α-sat) motifs of a 171 bp DNA sequence.[5−7] It is a biologically relevant sequence that is tandemly repeated hundreds to thousands of times, comprising 0.2−5 Mb stretches depending on the chromosome.[8−10]

$H3_{nuc}$ nucleosomes are composed of 147 bp DNA wrapped around a protein core of histone proteins (H2A, H2B, H3, and H4) and condense the genome into a more manageable structure.[11−13] This compact structure is essential for protecting the genome from damage and plays a critical role in gene regulation.[14−17]

In centromeric CENP-A octameric nucleosomes, H3 histones are replaced with CENP-A histones, an H3 homologue.[1,10,18−20] These two homologues share a 50% homology in the C-terminal histone fold domain but vary drastically in the N-terminal tail in both size and sequence.[21,22] These and other structural differences between CENP-A and H3 result in an unfixed 13 bp at both entry/exit of the CENP-A nucleosome, so centromeric CENP-A_{nuc} octameric nucleosomes wrap ∼20 bp less DNA than bulk H3 nucleosome.[23,24]

Studies show that transcription does occur in the centromere, yielding different products depending on the number of repeats of α-sat.[25,26] The transcription occurring in the centromere yields lncRNAs, which functionally load both CENP-A and CENP-C.[20] However, there is a 200−300 fold difference between bulk chromatin and centromere transcription.[10,20,27]

The accessibility of transcription factors to the bulk vs centromere chromatin may be one of the explanations, so to test this hypothesis, we investigated the interaction of NF-κB transcription factor with both types of nucleosomes. NF-κB is a transcription factor that recognizes κB sites in the DNA and is crucial in regulating the immune response and inflammation. The α-sat sequence contains many half κB sites, which are also known to bind NF-κB.[10,20,28,29] We previously reported that NF-κB binds and unravels $H3_{nuc}$ nucleosomes assembled with the Widom 601 DNA motif.[30] Here, we tested how NF-κB interacts

Received: December 24, 2023
Revised: May 31, 2024
Accepted: May 31, 2024

with nucleosomes assembled on the centromere-specific a-sat sequence. Both $H3_{nuc}$ and CENP-A_{nuc} were assembled on the same DNA substrate, and the interaction of the nucleosomes with NF-κB was studied using AFM. The analysis of AFM data revealed that NF-κB unravels $H3_{nuc}$ but does not appear to bind or unravel CENP-A_{nuc} nucleosomes.

EXPERIMENTAL METHODS

DNA Preparation. The DNA construct was prepared the same way that we had done previously.[30−32] The alpha satellite-containing construct was made using PCR with a pUC57 plasmid vector from BioBasic (Markham, ON, CA). The DNA total sequence was 410 bp, with the alpha satellite sequence in the middle. The specific sequence used is 5′- GATGTGCTG-CAAGGCGATTAAGTTGGGTAACGCCAGGGTTTTCC-CAGTCACGACGTTGTAAAACGACGGCCAGTGAATTC-GAGCTCGGTACCTCGCGAATGCATCTAGATGAC-CATTGGATTGAACTAACAGAGCTGAACACTCCTTTA-GATGGAGCAGATTCCAAACACACTTTCTGTA-GAATCTGCAAGTGGATATTTGGACTTCTCTGAG-GATTTCGTTGGAAACGGGATAAAATTCCCAGAACTA-CACGGAAGCATTCTCAGAAACTTCTTTGTGAT-GAAGGGCGAATTCGAATCGGATCCCGGGCCCGTC-GACTGCAGAGGCCTGCATGCAAGCTTGGCGTAAT-CATGGTCATAGCTGTTTCCTGTGTGAAATTGT-TATCCGCTCACAATTCCACACAACATACG −3′. After the PCR amplification of the DNA substrate, the DNA was concentrated and purified using the Gel Extraction Kit from Qiagen (Hilden, DE). Lastly, the DNA concentrations were calculated using a NanoDrop Spectrophotometer (ND-1000, Thermo Fischer).

Preparation of Proteins (NF-κB). N-terminal hexahistidine murine $p50_{39-350}$/$RelA_{19-321}$ (hereafter referred to as NF-$κB_{RHD}$) was expressed using a modified pET22b vector containing the genes for both polypeptides as described previously.[33] The DNA for murine RelA residues 19−549 was synthesized and subcloned into a modified pET22b vector which already contained the gene for N-terminal hexahistidine-$p50_{39-350}$ (hereafter referred to as NF-$κBA_{FL}$). The DNA sequence of $RelA_{TAD}$ (RelA residues 340−549) was subcloned into pET28a vector with a C-terminal hexahistidine tag.

All vectors were transformed into *E. coli* BL-21 (DE3) cells and grown with an OD_{600} of 0.5−0.7 at 37 °C in M9 minimal media with antibiotic selection. Cultures were cooled on ice for 20 min, then protein expression was initiated by the addition of 0.2 mM IPTG. Cultures were incubated at 18 °C for 16 h, then harvested by centrifugation. Pellets were stored at −80 °C.

The NF-$κB_{RHD}$, NF-$κB_{FL}$, and $RelA_{TAD}$ constructs were lysed by sonication and purified by Ni^{2+}-NTA chromatography as described previously for NF-$κB_{RHD}$,[30] an SDS Page gel and electrophoretic mobility shift assay images of NF-κB can be seen in Figure S1. Following overnight dialysis, the protein was aliquoted and stored at −80 °C. Prior to experiments, aliquots were thawed and further purified. NF-$κB_{RHD}$ and NF-$κB_{FL}$ were purified by cation exchange chromatography (MonoS; GE healthcare) to remove bound nucleic acids, as described previously.[30] Protein was further purified by size-exclusion chromatography using a Superdex 200 column (GE healthcare) in SEC buffer (25 mM Tris, 150 mM NaCl, 0.5 mM EDTA, 1 mM DTT, adjusted to pH 7.5 at room temperature). Care was taken to separate NF-$κB_{FL}$ from a breakdown product that eluted at the same volume as NF-$κB_{RHD}$. $RelA_{TAD}$ was purified by size-exclusion chromatography using a Superdex 75 column, followed by a Superdex 200 column (GE healthcare) in the same buffer.

All purification chromatography steps were conducted in a 4 °C cold room. Purity of all proteins was assessed by SDS-PAGE. The protein concentration was determined by absorption at 280 nm using a NanoDrop spectrophotometer. Purified protein was stored at 4 °C and all experiments were conducted within 72 h of purification by size exclusion chromatography.

NF-κB Reaction. The addition of NF-κB to DNA or nucleosome-containing samples was completed in the same manner as previously.[30] The NF-κB was diluted to 300 nM for nucleosome experiments and 600 nM for DNA experiments in NF-κB buffer (25 mM Tris pH 7.5, 150 mM NaCl, 0.5 mM EDTA, 1 mM DTT). The DNA experiments incubated NF-κB at a 2:1 ratio with the DNA for 10 min at room temperature. The nucleosome experiments incubated NF-κB at a 1:1 ratio, resulting in 150 nM for both nucleosomes and NF-κB, and incubated for 10 min at room temperature.

Nucleosome Assembly. The nucleosome assembly utilizes a previously used method of dialyzing from a high salt concentration (2 M) to a low salt concentration of 2.5 mM.[24] Our nucleosome assembly begins with an initial buffer (10 mM Tris pH 7.5, 2 M NaCl, 1 mM EDTA, 2 mM DTT), in which we incubate the nucleosome octamers purchased from The Histone source (Fort Collins, CO) in a dialysis tube for 1 h to allow the glycerol concentration to decrease. Following the initial 1 h incubation at 4 °C, we begin pumping the secondary buffer (10 mM Tris pH 7.5, 2.5 mM NaCl, 1 mM EDTA, 2 mM DTT) into the initial buffer using a peristaltic pump, which simultaneously pumps the initial buffer out, maintaining a consistent volume. The changing of NaCl concentration occurs for 24 h at 4 °C. After 24 h, another 1-h incubation occurs in the secondary buffer to ensure the final concentration of NaCl is 2.5 mM. CENP-A_{nuc} requires an additional step of adding in 1:2 tetramer:dimer molar concentrations for a proper octamer assembly. The CENP-A/H4 tetramer and H2A/H2B dimer are ordered from EpiCypher (Durham, NC).

AFM Imaging. The preparation of the samples was completed as performed previously by our lab.[30,31] The nucleosomes were stored at 300 nM, and the imaging of nucleosomes was completed at 2 nM. A dilution in our imaging buffer (4 mM $MgCl_2$ and 10 mM HEPES) down to 2 nM was achieved for the control samples before the deposition. For samples that contain NF-κB, a mixture of the stock nucleosome sample and the NF-κB was done at the highest possible concentration. The 300 nM nucleosome stock was mixed with a 1:1 or 1:2 DNA: NF-κB ratio and incubated at room temperature for 10 min before diluting and preparing for deposition. AFM samples were deposited on functionalized APS mica, incubated for 2 min, washed with DI water, and gently dried under argon flow. Samples were stored in a vacuum before being imaged on a Multimode AFM/Nanoscope IVD system using TESPA probes (Bruker Nano Inc., Camarillo, CA).

Data Analysis. Data analysis was completed using previously successful techniques in our lab.[30] The contour length measurements were conducted using Femtoscan (Advance Technologies Center, Moscow, Russia). The measurements started at the DNA's end and ended in the middle of the protein (nucleosome or NF-κB). Then, the other DNA flank was measured. 5 nm was subtracted from each DNA flank to account for the length contributed by the histone core. The measurements were measured in nm and converted into bp through a conversion factor calculated by measuring naked

https://doi.org/10.1021/acs.jpcb.3c08388
J. Phys. Chem. B XXXX, XXX, XXX−XXX

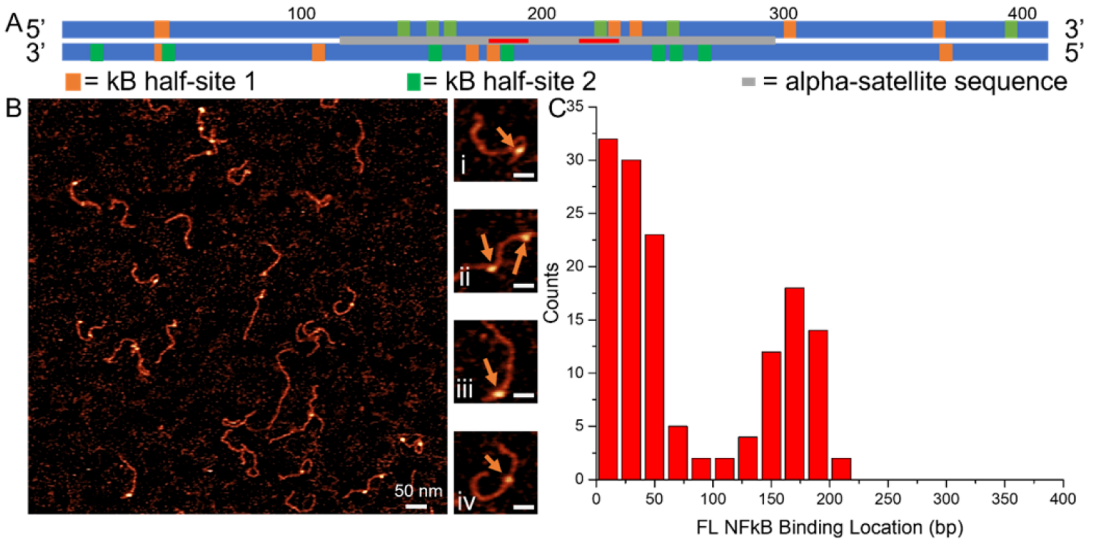

Figure 1. DNA Construct and AFM image with NF-κB_{FL} results. (A) DNA construct containing the alpha-satellite sequence in the middle of the sequence (gray bar), to analyze if there was any preferential binding at half sites, they are displayed in the "forward" 5′ → 3′ direction and again in "reverse" 3′ →5′, and the half-sites were marked (green and orange). The κB half-sites 1 (GGGRN) were labeled with orange boxes, and the κB half-sites 2 (YYYCC) were labeled with green boxes. The CENP-B box was marked in red. (B) AFM images of DNA with NF-κB_{FL} at a 1:2 molar ratio. Snapshots shown to the right of large AFM images (i), (iii), and (iv) show a single NF-κB_{FL} bound to the DNA, and image (ii) shows two NF-κB_{FL} bound to the DNA. The orange arrows indicate an NF-κB_{FL} bound to the DNA. The large AFM image is a 1 × 1 μm^2 scan size with a 50 nm scale bar. The snapshots are 100 × 100 nm^2 scan area and 25 nm scale bars. (C) The histograms for binding location for a single NF-κB_{FL}, indicating a preference for terminal and middle part of the DNA construct (a second peak around ∼170 bp).

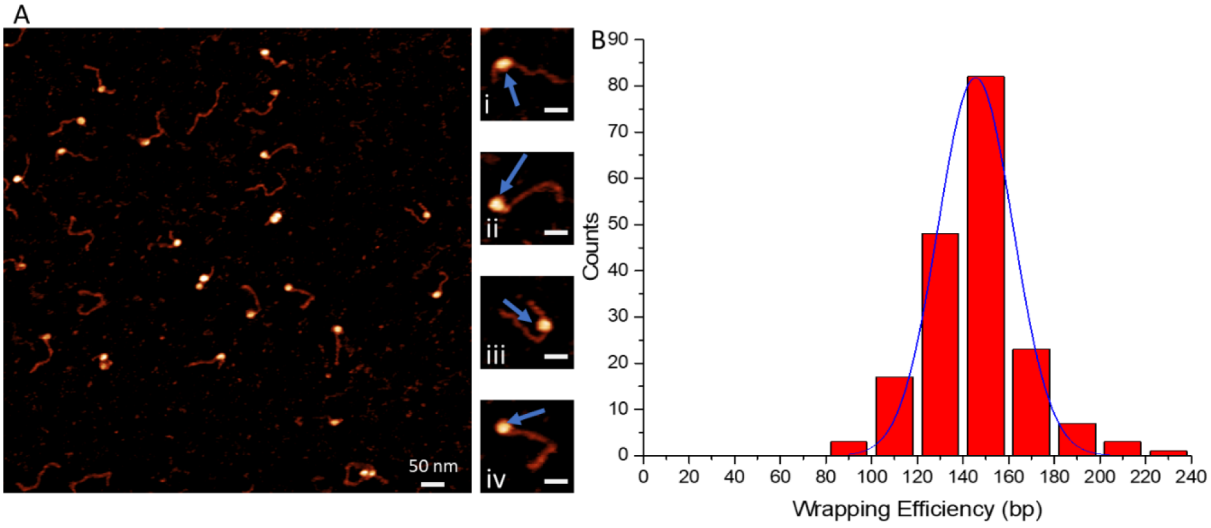

Figure 2. AFM image with zoomed-in snapshots of canonical $H3_{nuc}$. (A) AFM images of the canonical $H3_{nuc}$ assembled on the DNA construct. The large AFM image is a 1 × 1 μm^2 scan size with a 50 nm scale bar. The snapshots to the right of the large AFM show the varying nucleosome binding locations. The snapshots are 100 × 100 nm^2 scan area and 25 nm scale bars. Snapshots (ii) and (iv) show terminally bound nucleosomes, and (i) and (iii) are closer to the middle but are not terminally bound. The blue arrows indicate the location of a nucleosome. (B) The wrapping efficiency of the nucleosomes on the DNA substrate was 146 ± 1.6 bp (SEM) shown as the histogram.

DNA on each image. We took the full-length measurement of naked DNA and divided it by the known bp of the DNA to get a conversion factor typically around 0.35 nm/bp. Once DNA measurements were completed, Origin (Originlab Corporation) software is used to fit the data into bins and the visual representation of histograms. Origin was used to calculate the mean Gaussian distributions of the histograms. The mapping of the nucleosomes utilized the two DNA flank measurements, and the short lengths were used to create bins. The nucleosome binding locations were created using Microsoft Excel from the bin information provided by Origin. The height was calculated in Femtoscan using grain analysis, and each nucleosome was individually selected. The height is calculated through the utilization of multiple cross sections.

RESULTS

NF-κB Binding to the Alpha Satellite DNA Substrate. In these studies, we used a DNA construct containing an alpha satellite (α-sat) sequence, 171 bp long, present exclusively in the centromere part of the chromosome flanked with the DNA segments that are not specific for nucleosome binding. Schematics of the DNA are shown in Figure 1A. α-sat segment

https://doi.org/10.1021/acs.jpcb.3c08388
J. Phys. Chem. B XXXX, XXX, XXX−XXX

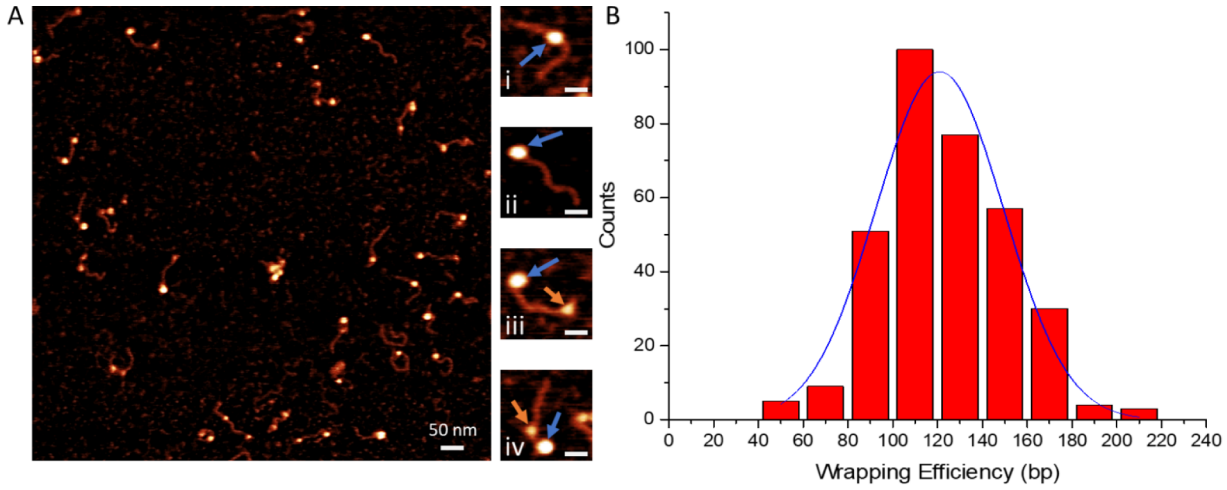

Figure 3. AFM image with zoomed-in snapshots of canonical $H3_{nuc}$with NF-κB_{FL}. (A) AFM images of $H3_{nuc}$ assembled on the DNA construct with NF-κB_{FL} added at a 1:1 ratio. The large AFM image is a 1×1 μm^2 scan size with a 50 nm scale bar. The snapshots to the right of the larger AFM image show varying situations. The snapshots are 100×100 nm^2 scan area and 25 nm scale bars. In (i) and (ii), there is a nucleosome bound near the center of the DNA, with no NF-κB visible. In (iii), the nucleosome is bound to one side of the DNA, and the NF-κB is bound to the other side. In (iv), there is a terminally bound nucleosome with an NF-κB_{FL} bound adjacently. The orange arrows indicate NF-κB_{FL} bound to the DNA, and the blue arrows indicate the nucleosome. (B) The histogram of the wrapping efficiency values measured for the NF-κB_{FL}−nucleosome complexes.

was placed in the middle of the construct, indicated with a gray bar below. Green and orange bars indicate the positions of the NF-κB half recognition sequences. Both the central α-sat segment and flanks contain NF-κB binding sites.

The DNA was complexed with NF-κB_{FL} using a 1:1 protein-to-DNA molar ratio and imaged with AFM. AFM images are shown in Figure 1B. Protein bound to DNA appears as a globular feature on the DNA filament. Similar to our previous study,[30] NF-κB does not alter the length of the DNA, suggesting that there is no wrapping DNA around the protein. A few zoomed images are displayed to the right (frames (i)−(iv)), and the protein position is indicated with arrows in these images. Complexes of the DNA with one or two NF-κB_{FL} molecules are seen, and both types of complexes are shown in selected frames. Protein can appear close to the end of the DNA (frames (i) and (iii)) or inside the DNA (frame (iv)). A similar arrangement was observed for two protein molecules bound to DNA (frames (ii)). Locations of the protein were mapped, and the results are shown as a histogram in Figure 1C. Two peaks correspond to the NF-κB_{FL} binding to the DNA ends (0−50 bp) and the central location (~170 bp). The mapping results correlate with NF-κB binding sites shown in Figure 1A. Note that the left and right ends of the DNA cannot be distinguished in the AFM images, so the end-bound peak corresponds to complexes of NF-κB with left−right binding sites on the DNA construct. Similarly, the peak at 170 bp corresponds to NF-κB bound to half-κB sites (green or orange bars) on both DNA strands between 100 and 200 bp and to 200−300 segments of the DNA. The binding affinity for NF-κB between the peaks is low, which is in line with the lack of NF-κB sites on both DNA strands in the construct. These results agree with other papers demonstrating the need for a half κB site for binding.[34,35]

Similar experiments were performed with the NF-κB_{RHD} variant in which the 228 amino acids of the TAD region were deleted. Regardless of the deletion, NF-κB_{RHD} demonstrates sequence-specific affinity very similar to the one for the full-length NF-κB heterodimer (Figure S2). These findings suggest that the C-terminal $RelA_{TAD}$ is not critical for the interaction of the NF-κB heterodimer with the DNA.

NF-κB Interaction with Canonical Nucleosomes $H3_{nuc}$.

Canonical nucleosomes $H3_{nuc}$ were assembled on the DNA substrate described above by the self-assembly process described in the methods section using an octameric histone core containing H2A, H2B, H3, and H4. The AFM images of nucleosomes are shown in Figure 2A, with a few selected frames to the right of the large scan. Nucleosomes are indicated with blue arrows. In addition to terminal locations in frames (ii) and (iv), nucleosomes occupy positions near the middle of the sequence (frames (i) and (iii)). The various positions of the nucleosomes located in the middle of the α-sat segment demonstrate that the α-sat segment is not a nucleosome-specific sequence. This conclusion aligns with our previous publication in which a similar DNA substrate was used.[31] We also measured another parameter of the nucleosome, the length of DNA wrapped around the core, termed the wrapping efficiency. This value was obtained by subtracting the lengths of the DNA not wrapped around the nucleosome core from the total length of the DNA. As shown in Figure 2B, the wrapping efficiency for the $H3_{nuc}$ sample is 146 ± 1.6 bp (SEM), which is in line with previous measurements on different DNA substrates, including the nucleosome-specific 601 motif.[30]

Next, we added NF-κB_{FL} to the assembled $H3_{nuc}$ sample in a 1:1 nucleosome:protein ratio, incubated the mixture for 10 min, and prepared the sample for AFM as in previous studies. AFM images are shown in Figure 3A, in which selected typical images of the complexes are shown to the right of the large AFM scan. Frame (i) shows just an $H3_{nuc}$ (blue arrows), frames (ii) and (iv) show a terminally bound $H3_{nuc}$ with an NF-κB_{FL} protein adjacent to it (orange arrows), and frame (iii) shows a terminally bound nucleosome with an NF-κB_{FL} on the opposite end of the DNA. The nucleosomes and NF-κB_{FL} can be visually differentiated based on their overall sizes, with NF-κB being significantly smaller than the nucleosome.

Next, we calculated the wrapping efficiency from these data as described above. The histogram from multiple measurements is shown in Figure 3B. The distribution was fit to a Gaussian distribution, yielding a mean value of the wrapping efficiency of 125 ± 2.2 bp (SEM). This number is considerably lower than

https://doi.org/10.1021/acs.jpcb.3c08388
J. Phys. Chem. B XXXX, XXX, XXX−XXX

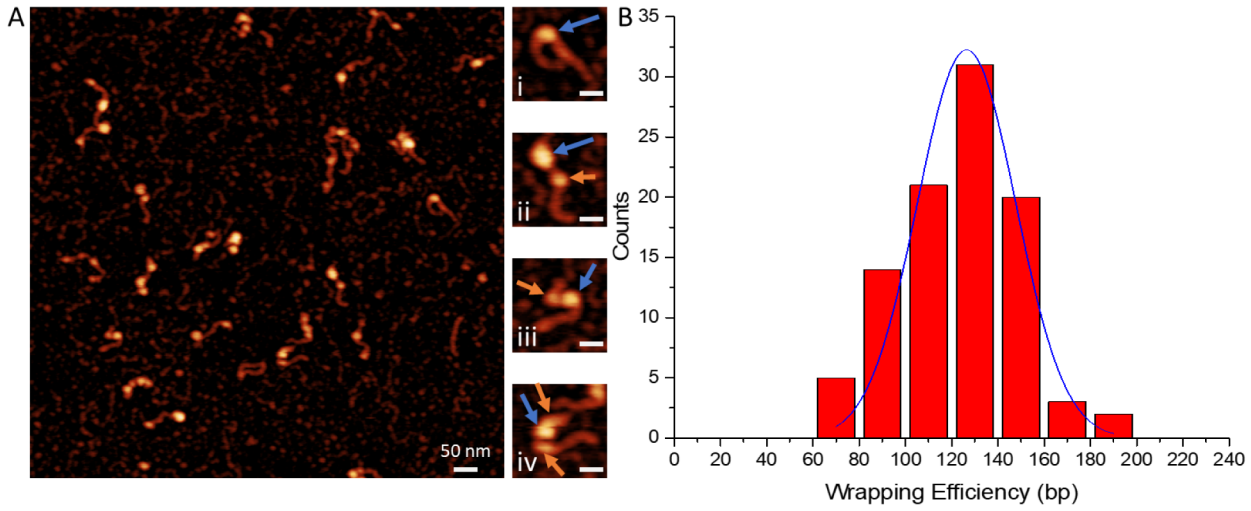

Figure 4. AFM image with zoomed-in snapshots of canonical $H3_{nuc}$ with NF-κB_{FL}. (A) AFM images of $H3_{nuc}$ assembled on the DNA construct with NF-κB_{FL} added at a 1:2 ratio. The large scan in (A) is 1×1 μm^2, and the scale bar is 50 nm. The snapshots to the right of the larger AFM image show varying situations. The snapshots are 100×100 nm^2, and the scale bar is 25 nm. In (i), there is a nucleosome bound near the center of the DNA. In (ii) and (iii), the nucleosome is bound to the DNA, and the NF-κB is bound near the nucleosome. In (iv), the nucleosome has an NF-κB_{FL} bound to both sides of the nucleosome. The orange arrows indicate NF-κB_{FL} bound to the DNA, and the blue arrows indicate the nucleosome. (B) The histogram of the wrapping efficiency values.

the wrapping efficiency of the control sample, 146 ± 1.6 bp (SEM). This suggests that in the presence of NF-κB_{FL}, the nucleosomes are unraveled by some 21 ± 3.8 bp (SEM). The p-value between these two populations was 9.6×10^{-10}, indicating a statistically significant difference between the control and the NF-κB_{FL} containing population.

We completed a parallel experiment that tested the effects of adding additional NF-κB to the nucleosome sample. In these experiments, we had a nucleosome: NF-κB ratio of 1:2 to check if increasing the concentration would affect the unwrapping effect of NF-κB. The AFM image can be seen in Figure 4A. In frame (i), a single nucleosome bound near the middle of the DNA can be seen. In frames (ii) and (iii), there is one $H3_{nuc}$ and one NF-κB_{FL}. In frame (iv), there is an $H3_{nuc}$ and two NF-κB_{FL} bound to both sides of the nucleosome. The histogram of the wrapping results can be seen in Figure 4B. The unwrapping effect of the nucleosomes resulted in a wrapping efficiency of 125 ± 2.6 bp (SEM) regardless of the increased ratio of NF-κB. The wrapping efficiency remains the same as in the previous experiments, but the yield of NF-κB bound to DNA flanks on the same strand as a nucleosome was calculated to be 43% and 85% for 1:1 and 1:2, respectively, which is in line with the use of higher concentration of NF-κB.

Although NF-κB bound to the nucleosome itself cannot be visualized with AFM directly, its contribution to the particle size can be evaluated with AFM by the height or volume measurements.[36] The height of NF-κB_{FL} bound to DNA was measured, as well as the DNA height on each AFM image. The results are shown in Figure S3. The average DNA height was subtracted from the height measurements of NF-κB_{FL} bound to the DNA and was found to be 0.55 ± 0.02 nm (SEM) (n = 82). The height measurements for the set of 183 particles for the $H3_{nuc}$ control produced the value 1.9 ± 0.02 nm (SEM). Similar measurements for the nucleosome particles (n = 157) in the presence of NF-κB led to the value 2.3 ± 0.04 nm (SEM), which is statistically significant from the control measurements. The p-value between these two populations was 5.4×10^{-23}, indicating a statistically significant difference between the control and the NF-κB_{FL} containing population. These data are summarized in Table 1.

Table 1. Results for Experiments with $H3_{nuc}$ with a Subpopulational Analysis of Under-wrapped Nucleosomes, all Nucleosome Samples, and with the Full-length NF-κB at a 1:1 Molar Ratio

H3 nucleosomes	under-wrapped control	overall control	NF-κB_{FL}
wrapping mean (bp)	129 ± 1.5	146 ± 1.6	125 ± 2.2
height mean (nm)	1.8 ± 0.03	1.9 ± 0.02	2.3 ± 0.04
volume mean (nm^3)	377 ± 15	355 ± 9	469 ± 9

We also completed a volume analysis of the control $H3_{nuc}$ and $H3_{nuc}$ in the presence of NF-κB_{FL}, which were found to be 355 ± 9.4 nm^3 (SEM) and 469 ± 9.0 nm^3 (SEM), respectively. Histograms of these results can be seen in Figure S4. The p-value between these two populations was 1.8×10^{-15}, indicating a statistically significant difference between the control and the NF-κB_{FL} containing population.

Similar studies were performed with truncated NF-κB_{RHD} protein. Images of the sample with snapshots can be seen inFigure S5A, where the nucleosomes are indicated with a blue arrow, and the NF-κB_{RHD} are marked with orange arrows. The snapshots from the larger AFM image can be seen to the right, where frames (i) and (iii) show nucleosomes in different places on the DNA. In frames (ii) and (iv), a nucleosome is either terminally bound or close to the end of the DNA with an NF-κB_{RHD} protein bound on the DNA flank. The wrapping efficiency of the complex was decreased to 126 ± 1.5 bp (SEM) (Figure S5B). This value is similar to the results obtained for the full-length NF-κB, suggesting that the C-terminal $RelA_{TAD}$ does not contribute to the unraveling property of NF-κB. The height measurements for the nucleosomes with NF-κB_{RHD} was 1.9 ± 0.02 nm (SEM)(Figure S4C). Given that DNA contributes to the nucleosome sizes, control measurements for the subpopulation of $H3_{nuc}$ with 129 ± 1.5 bp wrapping efficiency were made. These measurements resulted in a height

https://doi.org/10.1021/acs.jpcb.3c08388
J. Phys. Chem. B XXXX, XXX, XXX−XXX

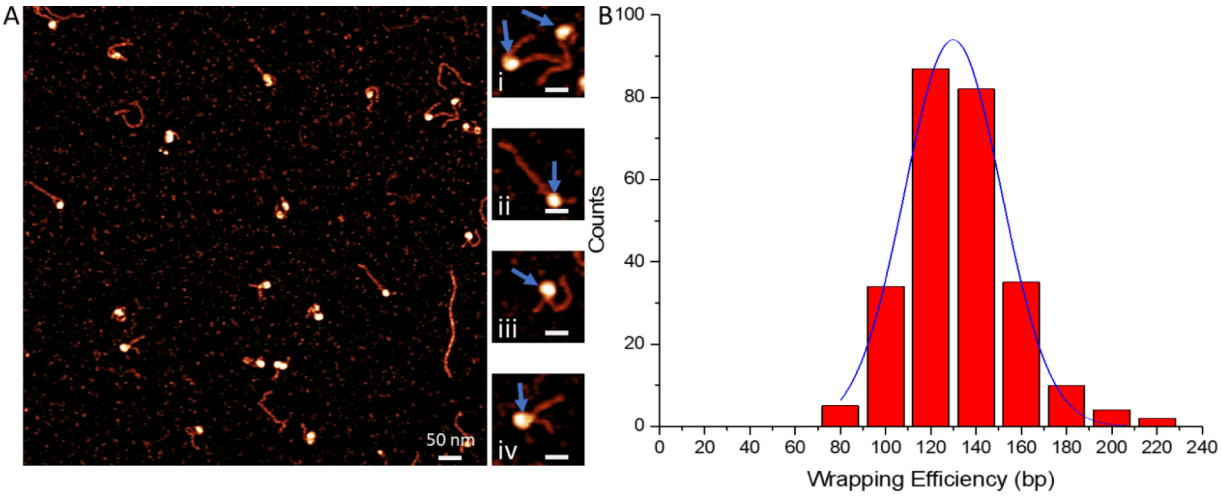

Figure 5. AFM image with zoomed-in snapshots of centromeric CENP-A_{nuc}. (A) AFM images of CENP-A_{nuc} assembled on the DNA construct. The large AFM image is 1 × 1 μm^2, and the snapshots are 100 × 100 nm^2. The scale bars are 50 and 25 nm for the large AFM image and snapshots, respectively. The snapshots to the right of the large AFM image show typical nucleosomes assembled on the DNA construct. In (i), there are two nucleosomes, one close to the end and one more centrally bound. In (ii) and (iii), nucleosomes are close to the terminal end. In (iv), the nucleosome is closer to the middle of the DNA. (B) The histogram of the wrapping efficiency approximated withthe Gaussian distribution. The scale bar is 50 and 25 nm for the large image and snapshots, respectively.

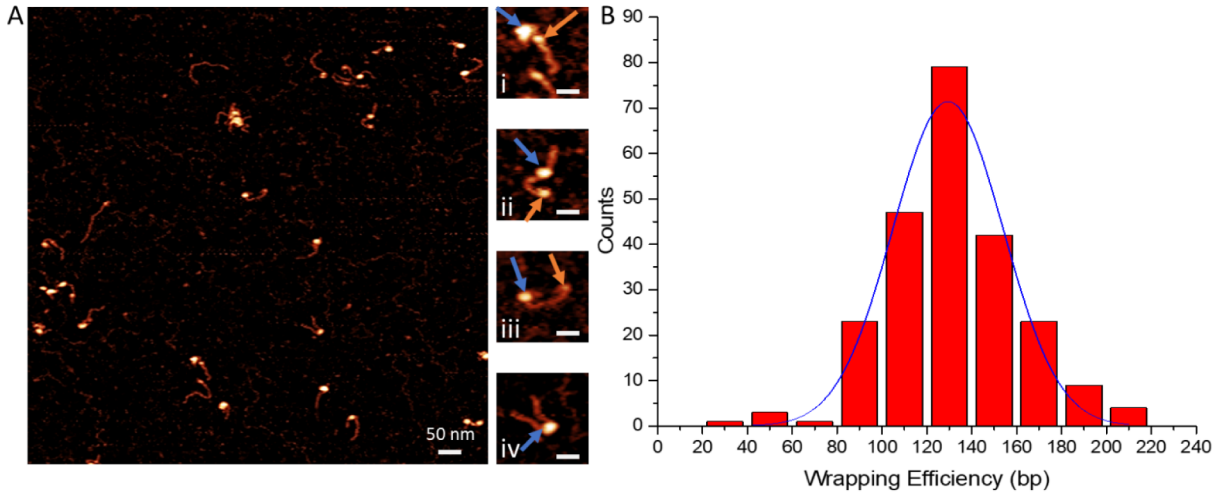

Figure 6. AFM data for the centromeric CENP-A_{nuc} with NF-κB_{FL}. (A) AFM images of CENP-A_{nuc} assembled on the DNA construct with 1:1 NF-κB_{FL}.The larger AFM image has a scan size of 1 × 1 μm^2, and the snapshots are 100 × 100 nm^2 and scale bars of 50 and 25 nm, respectively. The snapshots to the right of the large AFM image have NF-κB_{FL} added to the assembled nucleosomes and can be seen easily, represented by the orange arrows. The blue arrows represent the nucleosomes. The snapshots show nucleosomes binding near the terminal and can be seen in (i) and (iii), whereas centrally bound nucleosomes can be seen in (ii) and (iv). (B) The histogram of wrapping efficiency.

of 1.8 ± 0.03 nm (SEM). This value is less than the height of complexes of NF-κB_{RHD} protein with nucleosome, suggesting that the truncated NF-κB_{RHD} can be bound to the nucleosome.

Therefore, NF-κB leads to a substantial unraveling of $H3_{nuc}$. The unraveling of nucleosome by NF-κB was reported in our recent publication,[30] in which the nucleosome-specific 601 motif was used, but in this case, NF-κB unwrapped the 601 DNA to a lesser extent, only 135 ± 3 bp (SEM). Our data obtained on the physiologically relevant DNA substrate indicate that the nucleosome unraveling is a property of NF-κB, but the effect quantitatively depends on the DNA sequence.

NF-κB Interaction with Centromeric CENP-A_{nuc}. Centromeric-specific CENP-A_{nuc} were assembled on the α-sat DNA substrate mentioned above (Figure 1A) in a similar manner as $H3_{nuc}$, with the exception that CENP-A_{nuc} requires an extra step in the self-assembly process of mixing 2:1 molar concentrations of the dimeric H2A/H2B and tetrameric CENP-A/H4 (see the Methods section for details). The AFM images of the nucleosomes are shown in Figure 5A, with a few snapshots selected to the right. The snapshots of the assembled CENP-A nucleosomes shown in frames (i) and (ii) show nucleosomes bound close to the DNA ends, and frames (iii) and (iv) show nucleosomes closer to the middle of the DNA sequence. The nucleosomes are indicated with blue arrows. The wrapping efficiency of the CENP-A_{nuc} was 130 ± 1.6 bp (SEM) (Figure 5B), which is in line with our previous publications in which 601 motif DNA substrate along with nonspecific DNA sequences were used.[23,24,30]

Next, NF-κB_{FL} was added to CENP-A_{nuc} in a nucleosome-to-protein molar ratio of 1:1. The AFM results from CENP-A_{nuc} and NF-κB_{FL} can be seen in Figure 6A, where selected complexes can be seen in the snapshots shown to the right of

https://doi.org/10.1021/acs.jpcb.3c08388
J. Phys. Chem. B XXXX, XXX, XXX−XXX

the large AFM image. In frame (i), CENP-A_{nuc} is bound near the end of the DNA, and NF-κB_{FL} is adjacent to CENP-A_{nuc}. In frame (ii), CENP-A_{nuc} is bound to the middle, with NF-κB_{FL} bound to the end of the DNA. In frame (iii), CENP-A_{nuc} and NF-κB_{FL} are bound to opposite ends of the DNA. Frame (iv) shows a CENP-A_{nuc} bound to the middle of the DNA, with no NF-κB_{FL} on the DNA flanks. The blue arrows indicate CENP-A_{nuc} and the orange arrows indicate NF-κB_{FL} bound to DNA flanks. The wrapping efficiency of the nucleosomes at a 1:1 ratio was calculated as described above, and the histograms of multiple measurements can be seen in Figure 6B. The mean wrapping efficiency was 129 ± 1.6 bp (SEM). The wrapping efficiency of the nucleosomes mixed with NF-κB_{FL} at a 1:2 ratio is shown inFigure S6A. In frame (i), a single CENP-A_{nuc} is bound to the DNA. In frames (ii) and (iii), there is a single CENP-A_{nuc} bound near the end of the DNA, with a single NF-κB_{FL} bound on the flank of the DNA. In frame (iv), there is an NF-κB_{FL} bound to both sides of CENP-A_{nuc}. The wrapping efficiency of the 1 to 2 experiments can be seen inFigure S6B, which resulted in a wrapping efficiency of 131 ± 2.3 bp (SEM). Both the 1:1 and 1:2 wrapping efficiencies were unchanged from the results found in the control sample, suggesting that in the presence of NF-κB, there is no unwrapping to CENP-A_{nuc}. The number of NF-κB on the DNA flanks with CENP-A_{nuc} was 46% and 80% for molar ratios of 1:1 and 1:2, respectively. The p-value between the control and the 1:1 NF-κB_{FL} wrapping populations was 0.49, indicating no difference between the control and the NF-κB_{FL} populations. This increased binding of NF-κB to DNA indicates at least twice as much NF-κB seen bound to the DNA, which does not include NF-κB that is potentially bound to the nucleosomes.

Next, we looked for evidence of NF-κB_{FL} binding to CENP-A_{nuc} through analysis of the nucleosome's measured heights, which can be seen in Figure S7A-C. The NF-κB_{FL} protein bound to the DNA, minus the height of the DNA, was measured and found to be 0.54 ± 0.03 nm (SEM). The CENP-A_{nuc} control nucleosomes had a height of 2.2 ± 0.02 nm (SEM), and with the addition of NF-κB_{FL}, the height was 2.2 ± 0.04 nm (SEM). The p-value for the height values between these two populations was 0.008, indicating little statistically significant difference between the control and the NF-κB_{FL} containing population. These results are in contrast with $H3_{nuc}$, where an increase could be seen from the control upon the addition of NF-κB_{FL}. With CENP-A_{nuc}, there was no increase in height with the addition of NF-κB_{FL}, indicating no NF-κB_{FL} binding to CENP-A_{nuc}.

We also completed a volume analysis of the control $H3_{nuc}$ and $H3_{nuc}$ in the presence of NF-κB_{FL}, which were found to be 351 ± 8.2 nm^3 (SEM) and 338 ± 4.9 nm^3 (SEM), respectively. A histogram distribution of these results can be seen inFigure S4C,D. The p-value between these two populations was 0.27, indicating little statistical difference between the control and the NF-κB_{FL} containing population. These data are summarized in Table 2.

Table 2. Results for Experiments with CENP-A_{nuc} with an Analysis of all Nucleosome Samples and with the Full-length NF-κB at a 1:1 Molar Ratio

CENPA nucleosomes	control	NF-κB_{FL}
wrapping mean (bp)	130 ± 1.4	129 ± 2.2
height mean (nm)	2.2 ± 0.02	2.2 ± 0.04
volume mean (nm^3)	351 ± 5	338 ± 8

Similar experiments were completed with NF-κB_{RHD}. Images and snapshots can be seen in Figure S8A. The snapshots can be seen to the right of the large AFM image. In frames (i) and (ii), CENP-A_{nuc} is bound to the DNA without any NF-κB_{RHD} bound to the flanks. In frames (iii) and (iv), CENP-A_{nuc} is bound near the terminal end of the DNA with NF-κB_{RHD} bound adjacent to CENP-A_{nuc}. The nucleosomes are indicated with a blue arrow, and NF-κB_{RHD} are marked with orange arrows. The wrapping efficiency of CENP-A_{nuc} with NF-κB_{RHD} was 129 ± 1.6 bp (SEM) (Figure S8B), indicating no unwrapping. The height of nucleosomes was measured in the NF-κB_{RHD} containing samples and found to be 1.9 ± 0.02 nm (SEM)(Figure S8C) for CENP-A_{nuc}. These results show that NF-κB does not unravel CENP-A_{nuc} nor bind to the nucleosome.

Comparison of Nucleosome Positioning with NF-κB. We mapped the position of the nucleosome in these complexes, as shown in Figure 7A−C. Interestingly, the data show a lower population of nucleosomes at the DNA end when NF-κB is bound. This value was reduced to 16% compared with 27% for the control, which decreased even more with a 1:2 ratio decreasing to 9%. These results suggest that NF-κB can cause displacement of the nucleosomes from the end of the DNA.

The mapping results of the CENP-A_{nuc} control and in the presence of NF-κB_{FL} can be seen in Figure 7D-F. The maxima in Figure 7 correspond to the locations of nucleosomes with arm lengths of ∼50−70 bp, which only partially covers the α-satellite motif. Such mapping data are in contrast with the nucleosome map assembled on the template with the 601 motif reported in our recent publication.[30] This finding leads us to conclude that α-satellite is not a highly specific DNA segment for the nucleosome assembly. There was no consistent change in the mapping profile for the CENP-A nucleosomes in the presence of NF-κB.

The mapping data of $H3_{nuc}$ with NF-κB_{RHD} is shown inFigure S9A, which is very close to the data obtained for the full-length NF-κB. Similarly, the CENP-A mapping results with NF-κB_{RHD} were comparable to the effects of NF-κB_{FL}, with 12% terminal binding compared to 18% (Figure S9B).

An analysis of the height compared to the position of the nucleosome showed no correlation between the two. A scatter plot of the comparison for $H3_{nuc}$ can be seen inFigure S10A-F. This indicates that nucleosome repositioning is not solely occurring when NF-κB is bound to the nucleosome itself but can also occur when NF-κB is bound at the flanking DNA.

We considered the possibility that the observed repositioning was actually a result of nucleosome removal. The results show that whether NF-κB was absent (control) or present at a nucleosome:protein ratio of 1:1 or 1:2, the yield of $H3_{nuc}$ was 62%, 62%, and 63%, respectively. These results indicate that NF-κB does not remove nucleosomes from the DNA, but rather translocates them away from the DNA ends. The yield analysis was also completed for CENP-A_{nuc}; the results were 70%, 67%, and 71% for control, 1:1, and 1:2, respectively.

DISCUSSION

Our major findings are summarized in Figure 8 (see also Table 1). According to the graph in Figure 8, NF-κB unravels canonical H3 nucleosomes, removing more than 20 bp DNA out of 147 bp total DNA wrapped around the nucleosome core. The unraveling of nucleosomes by NF-κB was reported in our recent publication.[30] However, nucleosomes were assembled on the highly specific 601 sequence in that publication, and a lower unwrapping effect was observed. Elevated stability of the

https://doi.org/10.1021/acs.jpcb.3c08388
J. Phys. Chem. B XXXX, XXX, XXX−XXX

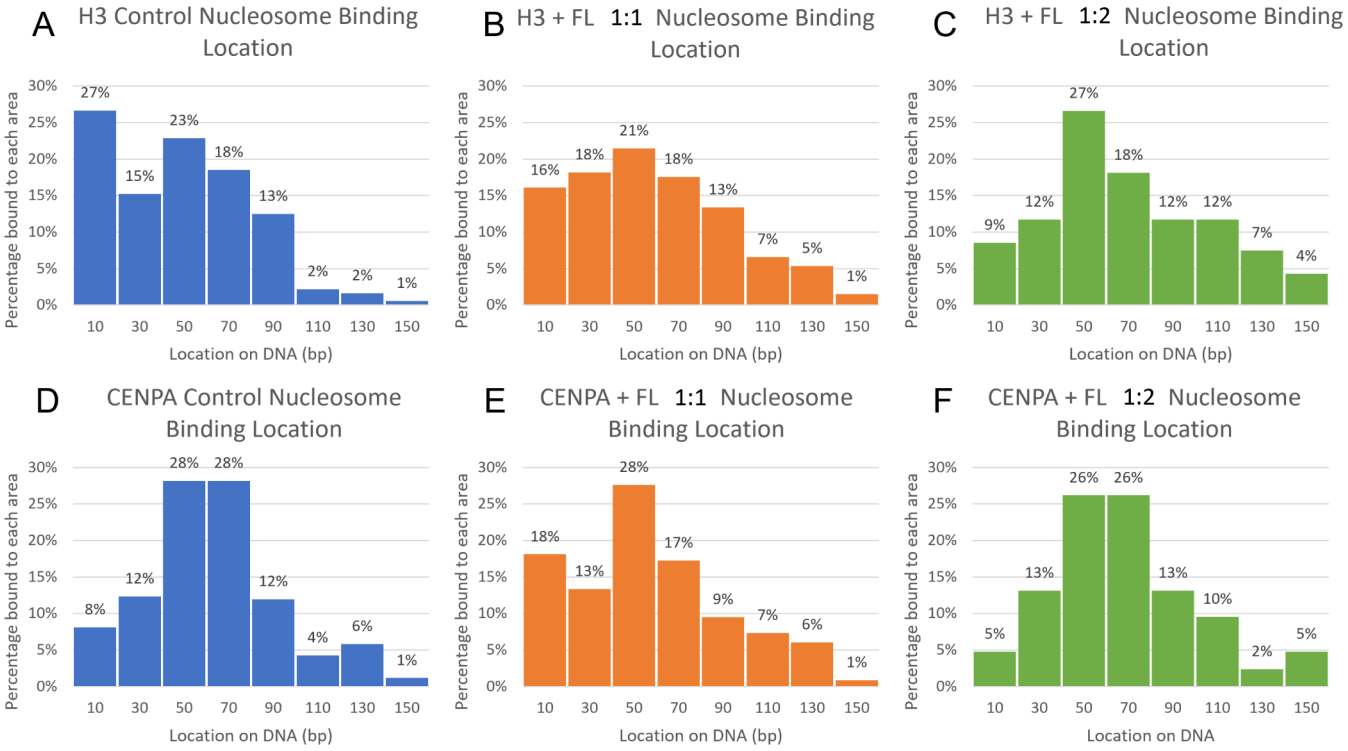

Figure 7. Nucleosome binding locations with varying concentrations of NF-κB_{FL}. Canonical nucleosome binding locations along the DNA construct: $H3_{nuc}$ Control (A), $H3_{nuc}$ with 1:1 NF-κB_{FL} (B), and $H3_{nuc}$ with 1:2 NF-κB_{FL} (C). The $H3_{nuc}$ control had a terminal binding percentage of 27%, drastically decreasing to 16% in samples with NF-κB_{FL}. The 1:2 NF-κB_{FL} had an end binding of 9%, an even greater decrease in terminal binding than the 1:1 sample. Centromeric nucleosome binding locations along the DNA construct: CENP-A_{nuc} control (D), CENP-A_{nuc} with 1:1 NF-κB_{FL} (E), and CENP-A_{nuc} with 1:2 NF-κB_{FL} (F). The CENP-A_{nuc} control had an end binding percentage of 8%, which was increased to 18% in samples with NF-κB_{FL}, at a 1:2 ratio, the terminal bound CENP-A_{nuc} decreased to 5%.

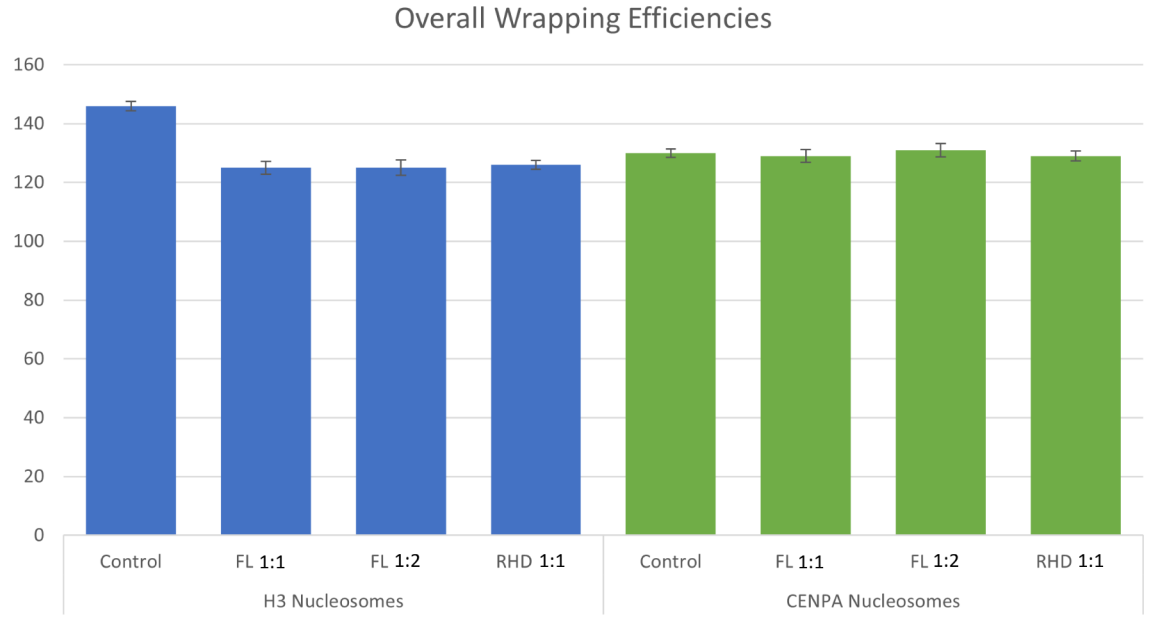

Figure 8. Effect of NF-κB on nucleosome wrapping efficiency. FL and RHD indicate the full-length and truncated variant NF-κB, respectively. The blue bars represent the $H3_{nuc}$ wrapping, the green bars represent the CENP-A_{nuc} wrapping, and the error bars show the SEM.

nucleosome assembled by the specific 601 DNA sequence can explain this effect.[37] Still, we need to consider the difference in the interaction of NF-κB with both DNA templates. The 601 motif contained only one κB binding site for NF-κB.[30] However, analysis of the NF-κB binding data did not reveal a preference for NF-κB binding at that site.[30] In contrast, the α-sat DNA substrate used in this work reveals a specific binding pattern of NF-κB (Figure 1). Importantly, the protein showed higher affinity for the DNA ends as well as for a cluster of half κB sites near the middle of the sequence. The affinity of NF-κB to the DNA ends can explain the decrease in the population of the end-bound nucleosomes in the presence of NF-κB by 1.5 times

https://doi.org/10.1021/acs.jpcb.3c08388
J. Phys. Chem. B XXXX, XXX, XXX−XXX

(Figure 7A−C). These observations suggest that binding of NF-κB to specific sites on DNA weakens nucleosome interactions, resulting in their displacement and/or dissociation. The findings in this paper on the similarity of nucleosome assembly on alpha-satellite and plasmid DNA sequences align with our previous findings.[23] Here, we found the elevated affinity of nucleosomes to the DNA ends, which is greater than the affinity to the alpha-satellite sequence, which could be related to other properties of the nucleosomes, such as their dynamics.

The $H3_{nuc}$ control had the highest wrapping efficiency at 146 ± 1.6 (SEM) bp, whereas $H3_{nuc}$ with NF-$κB_{FL}$ 1:1, NF-$κB_{FL}$ 1:2, and NF-$κB_{RHD}$ 1:1 had a lower wrapping at 125 ± 2.2 (SEM) bp, 125 ± 2.6 (SEM) bp, and 126 ± (SEM) 1.5 bp, respectively. The CENP-A_{nuc} results were very different from $H3_{nuc}$ with NF-κB not affecting the wrapping efficiency: the CENP-A_{nuc} control (130 ± 1.3 [SEM] bp), with 1:1 NF-$κB_{FL}$ (129 ± 2.2 [SEM] bp), with 1:2 NF-$κB_{FL}$(131 ± 2.3 [SEM] bp), and with 1:1 NF-$κB_{RHD}$ (129 ± 1.6 [SEM] bp).

Similar results of unraveling nucleosomes by NF-κB were obtained for the truncated variant NF-$κB_{RHD}$ (Figure S3), suggesting that the RelA C-terminal TAD does not define the unwrapping property of NF-κB. Given that the full-length NF-κB and its truncated variant NF-$κB_{RHD}$ have similar DNA binding patterns (Figure S2), we hypothesize that the DNA binding affinity of NF-κB is the factor defining the nucleosome unraveling property of NF-κB. We hypothesize that NF-κB binds to transiently dissociated DNA segments formed during the breathing of the nucleosome, stabilizing such an open state of the nucleosome and shifting the location of the nucleosome, explaining the repositioning of the population of the end-bound nucleosomes in the presence of NF-κB.

We displayed the effect of wrapping vs nucleosome height with and without NF-κB in Figures S11 and S12. The trend typically seen is that a lower height usually indicates a lower wrapping. The interaction of NF-κB with CENP-A nucleosomes is entirely different. As seen in Figures 3, 4, 6, and Figure S5, nucleosome wrapping remains unchanged, suggesting that regardless of the same affinity of NF-κB to DNA, the protein cannot unravel the CENP-A nucleosome. A broader wrapping efficiency can be seen in the populations with NF-κB. This effect is likely due to a small subpopulation of nucleosomes that remain canonically wrapped and have not experienced the NF-κB unwrapping effect. Therefore, we have two populations: the first, and larger population, is unwrapped due to NF-κB, and the second is the canonical wrapping. The combination of both populations has the effect of a broader histogram for the wrapping efficiency. Mixing of NF-κB with nucleosomes in the 1:1 ratio sometimes results in the binding of two proteins to one nucleosome; this is statistically what would be expected. Our experimental data clearly demonstrate this with complexes of the DNA substrate with NF-κB only. There were complexes with two or even three NF-κB bindings to a single DNA, as well as complexes with no NF-κB binding (Figure 1), indicating that there can be one NF-κB bound to the DNA and another bound to the nucleosome, while others have no NF-κB binding. In Figures 3, 4, and 6, we intentionally showed AFM images with NF-κB and nucleosomes visible as an internal control for NF-κB presence. The volume and height measurements carried out on hundreds of observed complexes show that NF-κB also binds to nucleosomes.

If breathing of nucleosomes is the pathway by which NF-κB unwraps the nucleosome, then NF-κB will bind to the transiently dissociated DNA segments. In that case, these data indicate that CENP-A nucleosomes are more stable than canonical H3 nucleosomes. According to the graph in Figures S7B,C, there are no changes in the CENP-A nucleosome, suggesting that NF-κB does not bind to it. This could be explained by the elevated stability of CENP-A nucleosomes compared with canonical ones.[24] The ability of CENP-A nucleosomes to resist the binding of the high-affinity NF-κB to DNA can be a factor contributing to findings that in vitro CENP-A chromatin was predominantly nonpermissive for transcription compared to H3 chromatin.[38] This finding is in line with previous results, which showed a 200−300 fold decreased transcriptional activity of centromeric chromatin, including NF-κB, compared to euchromatin.[27]

■ ASSOCIATED CONTENT

Supporting Information

The Supporting Information is available free of charge at https://pubs.acs.org/doi/10.1021/acs.jpcb.3c08388.

Additional experimental AFM results and analysis, as well as height and volume analysis for both $H3_{nuc}$ and CENP-$A_{nuc.}$ Comparative analysis of nucleosome height vs position on the DNA and height vs wrapping of nucleosomes (PDF)

■ AUTHOR INFORMATION

Corresponding Authors

Elizabeth Komives − *Department of Chemistry and Biochemistry, UC San Diego, La Jolla, California 92093-0378, United States;* orcid.org/0000-0001-5264-3866; Email: ekomives@ucsd.edu

Yuri Lyubchenko − *Department of Pharmaceutical Sciences, University of Nebraska Medical Center, Omaha, Nebraska 68198-6025, United States;* orcid.org/0000-0001-9721-8302; Email: ylyubchenko@unmc.edu

Authors

Shaun Filliaux − *Department of Pharmaceutical Sciences, University of Nebraska Medical Center, Omaha, Nebraska 68198-6025, United States*

Chloe Bertelsen − *Department of Pharmaceutical Sciences, University of Nebraska Medical Center, Omaha, Nebraska 68198-6025, United States*

Hannah Baughman − *Department of Chemistry and Biochemistry, UC San Diego, La Jolla, California 92093-0378, United States*

Complete contact information is available at: https://pubs.acs.org/10.1021/acs.jpcb.3c08388

Author Contributions

S.F. designed research, performed research, analyzed data, and wrote the paper. C.B. performed research and analyzed data. H.B. contributed proteins and wrote the paper. E.K. designed research, analyzed data and wrote the paper. Y.L. designed research, analyzed data, and wrote the paper.

Funding

This work was supported by National Science Foundation (grants MCB 1941049 and 2123637 to Y.L.L.) and National Institutes of Health (GM100156-05A1 to B. K. and Y.L.L.).

Notes

The authors declare no competing financial interest.

■ ACKNOWLEDGMENTS

We thank L. Shlyakhtenko (University of Nebraska Medical Center) for useful insights and all of the Y.L.L. lab members for fruitful discussions of the data.

■ ABBREVIATIONS

AFM	atomic force microscopy
CENP-A_{nuc}	CENP-A containing nucleosomes
$H3_{nuc}$	H3 containing nucleosomes
NF-κB	nuclear factor kappa-light-chain-enhancer of activated B cells
NF-$κB_{FL}$	full length NF-κB
NF-$κB_{RHD}$	NF-κB with the RHD removed
SEM	standard error of the mean
TAD	transcription activation domain

■ REFERENCES

(1) McKinley, K. L.; Cheeseman, I. M. The Molecular Basis for Centromere Identity and Function. *Nat. Rev. Mol. Cell Biol.* **2016**, *17* (1), 16−29.
(2) McAinsh, A. D.; Meraldi, P. The CCAN Complex: Linking Centromere Specification to Control of Kinetochore-Microtubule Dynamics. *Semin. Cell. Dev. Biol.* **2011**, *22* (9), 946−952.
(3) Talbert, P. B.; Henikoff, S. What Makes a Centromere? *Exp. Cell Res.* **2020**, *389* (2), 111895.
(4) Gambogi, C. W.; Black, B. E. The Nucleosomes That Mark Centromere Location on Chromosomes Old and New. *Essays Biochem.* **2019**, *63* (1), 15−27.
(5) Alexandrov, I.; Kazakov, A.; Tumeneva, I.; Shepelev, V.; Yurov, Y. Alpha-Satellite DNA of Primates: Old and New Families. *Chromosoma* **2001**, *110* (4), 253−266.
(6) McNulty, S. M.; Sullivan, B. A. Alpha Satellite DNA Biology: Finding Function in the Recesses of the Genome. *Chromosome Res.* **2018**, *26* (3), 115−138.
(7) Willard, H. F. *Chromosome-Specific Organization Of Human Alpha Satellite DNA*. *Am J Hum Genet* **1985**, *37*, 524−532.
(8) Aldrup-MacDonald, M. E.; Kuo, M. E.; Sullivan, L. L.; Chew, K.; Sullivan, B. A. Genomic Variation within Alpha Satellite DNA Influences Centromere Location on Human Chromosomes with Metastable Epialleles. *Genome Res.* **2016**, *26* (10), 1301−1311.
(9) Rosandić, M.; Paar, V.; Basar, I.; Glunčić, M.; Pavin, N.; Pilaš, I. CENP-B Box and pJα Sequence Distribution in Human Alpha Satellite Higher-Order Repeats (HOR). *Chromosome Res.* **2006**, *14* (7), 735−753.
(10) Smurova, K.; De Wulf, P. Centromere and Pericentromere Transcription: Roles and Regulation··· in Sickness and in Health. *Front. Genet.* **2018**, *9*, 674.
(11) Cutter, A. R.; Hayes, J. J. A Brief Review of Nucleosome Structure. *FEBS Lett.* **2015**, *589* (20PartA), 2914−2922.
(12) McGhee, G. R. J.*Neues Jahrbuch für Geologie Und Paläontologie*E. Schweizerbart1980155184
(13) Zhou, B.-R.; Yadav, K. N. S.; Borgnia, M.; Hong, J.; Cao, B.; Olins, A. L.; Olins, D. E.; Bai, Y.; Zhang, P. Atomic Resolution Cryo-EM Structure of a Native-like CENP-A Nucleosome Aided by an Antibody Fragment. *Nat. Commun.* **2019**, *10* (1), 2301.
(14) Luger, K.; Mäder, A. W.; Richmond, R. K.; Sargent, D. F.; Richmond, T. J. Crystal structure of the nucleosome core particle at 2.8 A resolution. *Nature* **1997**, *389*, 251−260.
(15) Park, Y.-J.; Luger, K. Structure and Function of Nucleosome Assembly proteins this Paper Is One of a Selection of Papers Published in This Special Issue, Entitled 27th International West Coast Chromatin and Chromosome Conference, and Has Undergone the Journal's Usual Peer Review Process. *Biochem. Cell Biol.* **2006**, *84* (4), 549−549.
(16) Poirier, M. G.; Oh, E.; Tims, H. S.; Widom, J. Dynamics and Function of Compact Nucleosome Arrays. *Nat. Struct. Mol. Biol.* **2009**, *16* (9), 938−944.
(17) Szerlong, H. J.; Hansen, J. C. Nucleosome distribution and linker DNA: connecting nuclear function to dynamic chromatin structure. *Biochem. Cell Biol.* **2011**, *89* (1), 24−34.
(18) Pidoux, A. L.; Allshire, R. C. The Role of Heterochromatin in Centromere Function. In *Philosophical Transactions of the Royal Society B: biological Sciences*; Royal Society, 2005; Vol. *360*, pp. 569579. .
(19) Stellfox, M. E.; Bailey, A. O.; Foltz, D. R. Putting CENP-A in Its Place. *Cell. Mol. Life Sci.* **2013**, *70* (3), 387−406.
(20) Arunkumar, G.; Melters, D. P. Centromeric Transcription: A Conserved Swiss-Army Knife. *Genes* **2020**, *11* (8), 911.
(21) Quénet, D.; Dalal, Y. The CENP-A Nucleosome: A Dynamic Structure and Role at the Centromere. *Chromosome Res.* **2012**, *20* (5), 465−479.
(22) Black, B. E.; Foltz, D. R.; Chakravarthy, S.; Luger, K.; Woods, V. L.; Cleveland, D. W. Structural Determinants for Generating Centromeric Chromatin. *Nature* **2004**, *430* (6999), 578−582.
(23) Stormberg, T.; Lyubchenko, Y. L. The Sequence Dependent Nanoscale Structure of CENP-A Nucleosomes. *Int. J. Mol. Sci.* **2022**, *23* (19), 11385.
(24) Stumme-Diers, M. P.; Banerjee, S.; Hashemi, M.; Sun, Z.; Lyubchenko, Y. L. Nanoscale Dynamics of Centromere Nucleosomes and the Critical Roles of CENP-A. *Nucleic Acids Res.* **2018**, *46* (1), 94−103.
(25) McNulty, S. M.; Sullivan, L. L.; Sullivan, B. A. Human Centromeres Produce Chromosome-Specific and Array-Specific Alpha Satellite Transcripts That Are Complexed with CENP-A and CENP-C. *Dev. Cell* **2017**, *42* (3), 226−240.e6.
(26) Quénet, D.; Dalal, Y. A Long Non-Coding RNA Is Required for Targeting Centromeric Protein A to the Human Centromere. *eLife* **2014**, *3*, No. e26016.
(27) Bergmann, J. H.; Jakubsche, J. N.; Martins, N. M.; Kagansky, A.; Nakano, M.; Kimura, H.; Kelly, D. A.; Turner, B. M.; Masumoto, H.; Larionov, V.; et al. Epigenetic Engineering: Histone H3K9 Acetylation Is Compatible with Kinetochore Structure and Function. *J. Cell Sci.* **2012**, *125* (2), 411−421.
(28) Gilmore, T. D. Introduction to NF-κB: Players, Pathways, Perspectives. *Oncogene* **2006**, *25* (51), 6680−6684.
(29) Hunter, C. J.; De Plaen, I. G. Inflammatory Signaling in NEC: Role of NF-κB, Cytokines and Other Inflammatory Mediators. *Pathophysiol.* **2014**, *21* (1), 55−65.
(30) Stormberg, T.; Filliaux, S.; Baughman, H. E. R.; Komives, E. A.; Lyubchenko, Y. L. Transcription Factor NF-κB Unravels Nucleosomes. *Biochim. Biophys. Acta, Gen. Subj.* **2021**, *1865* (9), 129934.
(31) Stormberg, T.; Vemulapalli, S.; Filliaux, S.; Lyubchenko, Y. L. Effect of Histone H4 Tail on Nucleosome Stability and Internucleosomal Interactions. *Sci. Rep.* **2021**, *11*, 1.
(32) Vemulapalli, S.; Hashemi, M.; Lyubchenko, Y. L. Site-Search Process for Synaptic Protein-Dna Complexes. *Int. J. Mol. Sci.* **2022**, *23*, 212.
(33) Sue, S.-C.; Cervantes, C.; Komives, E. A.; Dyson, H. J. Transfer of Flexibility between Ankyrin Repeats in IκBα upon Formation of the NF-κB Complex. *J. Mol. Biol.* **2008**, *380* (5), 917−931.
(34) Mulero, M. C.; Wang, V. Y.-F.; Huxford, T.; Ghosh, G. Genome Reading by the NF-κB Transcription Factors. *Nucleic Acids Res.* **2019**, *47* (19), 9967−9989.
(35) Siggers, T.; Chang, A. B.; Teixeira, A.; Wong, D.; Williams, K. J.; Ahmed, B.; Ragoussis, J.; Udalova, I. A.; Smale, S. T.; Bulyk, M. L. Principles of Dimer-Specific Gene Regulation Revealed by a Comprehensive Characterization of NF-κB Family DNA Binding. *Nat. Immunol.* **2012**, *13* (1), 95−102.
(36) Konrad, S. F.; Vanderlinden, W.; Frederickx, W.; Brouns, T.; Menze, B. H.; De Feyter, S.; Lipfert, J. High-Throughput AFM Analysis Reveals Unwrapping Pathways of H3 and CENP-A Nucleosomes. *Nanoscale* **2021**, *13* (10), 5435−5447.
(37) Wang, Y.; Stormberg, T.; Hashemi, M.; Kolomeisky, A. B.; Lyubchenko, Y. L. Beyond Sequence: Internucleosomal Interactions Dominate Array Assembly. *J. Phys. Chem. B* **2022**, *126* (51), 10813−10821.

https://doi.org/10.1021/acs.jpcb.3c08388
J. Phys. Chem. B XXXX, XXX, XXX−XXX

(38) Sharma, A. B.; Dimitrov, S.; Hamiche, A.; Van Dyck, E. Centromeric and Ectopic Assembly of CENP-A Chromatin in Health and Cancer: Old Marks and New Tracks. *Nucleic Acids Res.* **2019**, *47* (3), 1051−1069.

https://doi.org/10.1021/acs.jpcb.3c08388
J. Phys. Chem. B XXXX, XXX, XXX−XXX